Electrical detection of ferromagnetic resonance in single layers of permalloy: Evidence of magnonic charge pumping

A. Azevedo,[1,*] R. O. Cunha,[1] F. Estrada,[1,3] O. Alves Santos,[1] J. B. S. Mendes,[1] L. H. Vilela-Leão,[1] R. L. Rodríguez-Suárez,[1,2] and S. M. Rezende[1]

[1]*Departamento de Física, Universidade Federal de Pernambuco, 50670-901, Recife, PE, Brasil*

[2]*Facultad de Física, Pontificia Universidad Católica de Chile, Casilla 306, Santiago, Chile*

[3]*Facultad de Biología, Universidad Michoacana de San Nicolás de Hidalgo, Av. Francisco J. Mújica S/N, Ciudad Universitaria, C. P. 58030, Morelia, Michoacán, Mexico*

(Received 24 February 2015; revised manuscript received 26 May 2015; published 2 July 2015)

The generation of a DC voltage in single layers of permalloy ($Ni_{81}Fe_{19}$) when the magnetization is undergoing ferromagnetic resonance is investigated in a series of samples with thickness varying from 4.0 to 150 nm. By sweeping the external field at a fixed microwave frequency, we measure a DC voltage at the ends of the layer as a function of the in-plane angle for each sample. The asymmetric voltage signal generated at the resonance field is a superposition of symmetric Lorentzian and antisymmetric Lorentzian derivative line shapes. The in-plane dependence of both symmetric and antisymmetric signals cannot be explained as due to spin rectification (SRE) only. The results are well explained by a model that takes into account in addition to the SRE the contribution of the recent discovered effect of magnonic charge pumping that converts magnetization dynamics into charge current by means of the spin orbit coupling.

DOI: 10.1103/PhysRevB.92.024402 PACS number(s): 85.75.−d, 75.70.Tj, 72.25.Pn, 76.50.+g

I. INTRODUCTION

The generation, manipulation, and detection of spin currents are significant concepts that are paving the way for the development of future spintronic devices. By injecting a spin-polarized electric current into a magnetic material, in which the local magnetization is noncollinear with the electron spins, it is possible to transfer torque to the magnetic media. Consequently, two different behaviors can occur: (i) a dynamical state in which the local magnetization experiences coherent precession or (ii) a static state in which the local magnetization simply switches from one static orientation to another [1]. This elegant effect, called spin-transfer torque (STT), is now used in commercially available devices. Furthermore, the reciprocal effect, which is the generation of spin current by magnetization precession, has been extensively investigated in ferromagnetic/nonmagnetic (FM/NM) bilayers driven to ferromagnetic resonance (FMR) by an external rf magnetic field. In this case the flow of spin angular moment with no flow of charge carriers allows the injection of a pure spin current in the adjacent NM material. This remarkable effect, called spin pumping effect (SPE), became very attractive for investigating pure-spin transport phenomena without interference from charge-based transport. SPE was theoretically proposed in 2002 [2] and was detected using different techniques such as the measurement of an additional source of magnetization damping [3], the detection of a dynamic exchange coupling in magnetic multilayers [4], and the measurement of a DC voltage along the NM layer in FM/NM bilayers [5]. The origin of the DC voltage was associated with the conversion of spin current into charge current at the NM layer by means of the inverse spin Hall effect (ISHE) [6–8].

It was shown [6] that a spin current density (in units of angular momentum/area time) $\vec{J}_S$ generates a charge current density $\vec{J}_C$ given by $\vec{J}_C = \theta_{SH}(2e/\hbar)\vec{J}_S \times \hat{\sigma}$, where θ_{SH} is the spin Hall angle and $\hat{\sigma}$ is the unit vector along the spin polarization. As electrical detection of the magnetization precession in FM/NM bilayers turned out to be a convenient technique to measure the flow of angular momentum into the NM layer, the interpretation of the DC voltage has posed many challenges. Whereas the conversion process of spin current into charge current, occurring at the NM material, is well understood as due to the spin-orbit interaction (SOI) scattering, the total measured electromotive force has been shown to be generated by a combination of different effects, such as ISHE, spin rectification, etc. [9–13]. As pointed out in Ref. [14], when different mechanisms combine to generate the electrical signal measured in FMR experiments, the inappropriate interpretation could explain in part the many different values reported by different groups for the same physical parameters extracted from data of similar experiments. Recently, a new ingredient has been added to this problem. It was discovered that ferromagnetic metals such as permalloy ($Ni_{81}Fe_{19}$ = Py) also exhibit ISHE and could be used as pure spin current detectors [15,16]. In addition, it has been found that single layers of Py driven to ferromagnetic resonance generate a DC voltage by themselves [17,18]. This discovery poses two major issues: (i) the origin of the underlying source of the self-induced voltage generated by single layers of Py under FMR condition and (ii) how this self-induced voltage affects the electrical measurements of the spin-pumping effect in FM/NM metallic bilayers. We are convinced that these two critical issues need to be well addressed to correctly interpret the electrical detection of FMR in metal bilayers.

Quite recently a different effect was reported that provides an efficient manner to electrically generate magnetic torque from orbital motion, i.e., from electric current: the relativistic spin-orbit torque (SOT) that was originally discovered in single layers of ferromagnets [19]. In this case the spin orbit interaction acts to constructively generate a spin accumulation

*Corresponding author: aac@df.ufpe.br

of the conduction electrons, causing a torque to be applied to the local magnetization of the ferromagnetic material. In order to produce spin accumulation, the properties of the material must be different for conduction electrons propagating in opposite directions, i.e., the materials need to exhibit broken inversion symmetry. This phenomenon can also occur in two-dimensional structures in which the inversion symmetry is broken in the transversal direction [20,21]. As happens for STT/SPE, and predicted by the Onsager reciprocity relations, there is a reciprocal phenomenon for the SOT, which is an electric charge generation from magnetization dynamics in single layer of ferromagnetic material. The reciprocal effect was very recently discovered and named magnonic charge pumping (MCP) [22]. The fundamental physics of MCP is the direct conversion of spin waves into charge current through the spin-orbit interaction. Thus, the FMR condition could be used as a prototype to investigate the magnonic charge pumping phenomenon in single layers of ferromagnetic materials that satisfy the aforementioned condition. The MCP effect can be generated by the excitation of the magnetization precession in ferromagnetic materials that exhibit lack of inversion symmetry, either bulk inversion symmetry breaking, that, for example, occurs in the zinc-blende crystal structure of (Ga,Mn)As, or the extrinsic structural inversion symmetry breaking perpendicular to its plane, which, for example, occurs in heterostructures comprising ferromagnetic thin layers. Unlike STT (or SPE), SOT (or MCP) does not need a second material to spin polarize the electric current (as required in STT) or a second material with high SOI to convert the pure spin current in charge current (as required in SPE). Therefore, materials with strong spin-orbit interaction could simplify the design of spintronic devices by using the SOT effect.

In this paper, we report the observation of the magnonic charge pumping effect in single layers of Py driven by FMR. DC voltages were measured, at the FMR condition, in a series of single films of Py with varying thicknesses. For each sample we analyze the in-plane angle dependence of the voltage line shape to separate the spin rectification effect from other sources. Comparison of the data with a theoretical model for the voltage including spin rectification leads to the conclusion that in single layers of Py the DC voltage measured can be well explained by adding a contribution from the magnonic charge pumping effect. The MCP contribution is mostly due to the surface anisotropy that is generated by the breaking of the inversion symmetry. By fitting the data with the model we were able to extract the spin-orbit parameter that couples magnetization dynamics to charge currents.

II. EXPERIMENTAL DETAILS

Our samples are of rectangular shape having lateral dimensions of 1.5 mm by 4.0 mm and thicknesses, t_{Py} varying from 4.0 to 150 nm. The samples were grown by DC sputtering on (100) Si substrates. Silver electrodes were sputtered at the ends of the samples by using shadow masks of 0.5 mm by 1.5 mm as illustrated in Fig. 1(b). The samples were mounted on the tip of a plastic rod and inserted through a hole drilled in the back wall of a rectangular microwave cavity operating in the TE_{102} mode, at 9.4 GHz with a Q

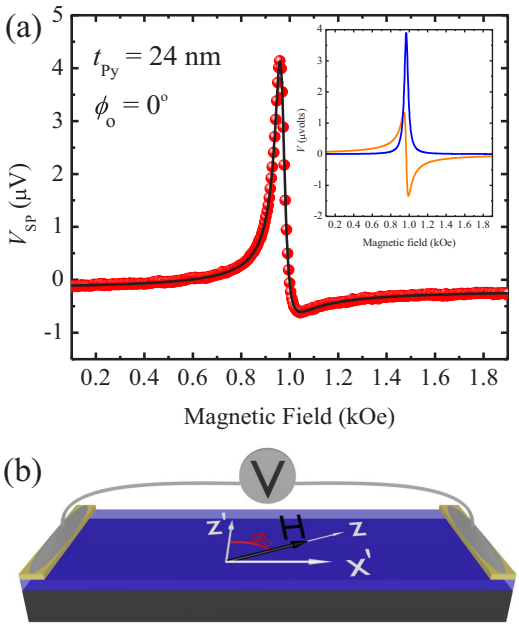

FIG. 1. (Color online) (a) Field sweep DC voltage measured for the sample with $t_{Py} = 34$ nm and for $\phi_o = 0°$. The black solid line was obtained by combining symmetric and antisymmetric Lorenztian curves that are shown in the inset. (b) Sketch of the sample setup including the reference frames used to interpret the data.

factor of 2000. By sweeping the external magnetic field a DC voltage is measured at the ferromagnetic resonance condition. The samples are placed in a nodal position of minimum rf electric field and maximum rf magnetic field. This precaution avoids the generation of galvanic effects driven by the rf electric field, thus the absorption of the rf magnetic field causes the magnetization precession. With this configuration our measurements are different from the spin rectification effect detected in single ferromagnetic films [23,24] in which both the rf electric and magnetic fields are directly applied to the sample.

In order to understand further the origin of the DC voltage generated in single layer of Py we investigated the angular dependence of the voltage for the complete series of films varying the thickness as described above. As is well known in spin pumping experiments using bilayers of FM/NM, the voltage measured along the NM layer can be interpreted as a superposition of the spin-pumping contribution (V_{SP}) and the spin rectification (V_{SRE}) contribution. In a previous paper [13] we showed that depending on the angular position, V_{SRE} has symmetric and antisymmetric components in field scan, whereas V_{SP} has only a symmetric component. For instance, for the magnetic field applied perpendicular to the direction of measurement, the line shape of the DC voltage is a pure Lorentzian curve, while for intermediate angles the line shape is made by a superposition of symmetric and antisymmetric components. Figure 1(a) shows a measurement of the DC voltage (red circles) obtained for the single layer of Py with thickness 24 nm and the magnetic field H_0 applied along the z' direction ($\phi_0 = 0°$), as defined in Fig. 1(b). Reference frame $x'z'$ is fixed on the sample, while the laboratory reference

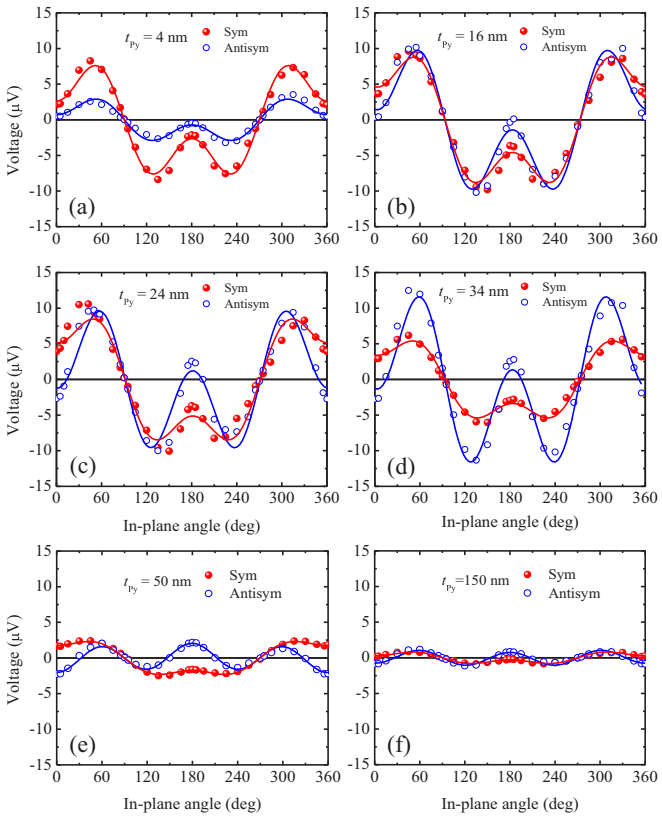

FIG. 2. (Color online) Angular dependence of the DC voltage amplitudes of the symmetric and antisymmetric Lorentzian curves, for some representative samples. The solid lines were obtained by adjusting the data (symbols) from the equations of the symmetric component, $A_{\rm sym}(\phi_0,H) = a_{\rm sym}\sin\phi_0\sin(2\phi_0) + b_{\rm sym}\cos\phi_0$ (red lines) and antisymmetric component, $B_{\rm antisym}(\phi_0,H) = a_{\rm antisym}\sin\phi_0\sin(2\phi_0) + b_{\rm antisym}\cos\phi_0$ (blue lines).

frame is defined by the plane xz. Axis y' (=axis y) is oriented down. Observe that the field scan voltage has an asymmetric line shape that can be fitted by a combination of symmetric Lorentzian and antisymmetric Lorentzian derivative functions given by

$$V(H) = V_{\rm sym}\Delta H^2/[(H-H_R)^2+\Delta H^2] + V_{\rm as}[\Delta H(H-H_R)]/[(H-H_R)^2+\Delta H^2].$$

Here $V_{\rm sym}$ and $V_{\rm as}$ denote, respectively, the amplitudes of the symmetric and antisymmetric components, while ΔH and $H_{\rm R}$ stand, respectively, for the FMR line width and resonance field. We decided to generically denote the amplitudes of the voltages by $V_{\rm sym}$ and $V_{\rm as}$, thus avoiding confusion with $V_{\rm SP}$ and $V_{\rm SRE}$ of our previous work [13]. The best fit to the data, shown by the black curve of Fig. 1(a), was obtained by the superposition of the symmetric (blue line in the inset) and antisymmetric (red line in the inset) components, for $V_{\rm sym} = 3.9 \pm 0.3\ \mu$V, $V_{\rm as} = -2.7 \pm 0.2\ \mu$V, $\Delta H = 24.5$ Oe, and $H_{\rm R} = 0.9677$ kOe. This result is an indication that the DC voltage generated in single layer of Py has a behavior that cannot be explained by the same approach used in Ref. [13], where $V_{\rm as}$ is null for the angles 0°, 90°, 180°, 270°. Figure 2 shows the angular dependence of $V_{\rm sym}$ and $V_{\rm as}$ for only six representative samples of the 18 samples investigated in which the thicknesses varied from 4.0 to 150 nm. As seen in Fig. 2, $V_{\rm sym}$ and $V_{\rm as}$ are null only for the angles $\phi_0 = 90°$ and $\phi_0 = 270°$, which cannot occur in bilayers of FM/NM as discussed in Refs. [13] and [14]. To explain this behavior we initially considered that, in addition to the x' component, the current density has a component in the z' direction. However, as will be shown below this consideration was not sufficient to explain the angular dependence of the $V_{\rm sym}$ and $V_{\rm as}$. Therefore, the DC voltage generated in single layer of Py under ferromagnetic resonance condition is in need of an additional source to be added to the SRE signal.

III. THEORETICAL INTERPRETATION AND RESULTS

In order to explain the additional source of DC voltage that is generated in single layers of Py under FMR, we developed a model that takes into account a contribution due to MCP that should be added to the contribution of SRE derived in Ref. [13]. We rule out the possibility that the charge current is due to the conversion of a spin current by the ISHE because the existence of this effect would require a nonuniform magnetization normal to the film plane and continuity provided by the contact of a spin sink material. As pointed in Ref. [22], the magnetic charge pumping effect can generate a DC voltage by averaging the time-dependent contribution, which is quadratic in the amplitude of the precessional angle and proportional to magnetization damping, so it must be orders of magnitude smaller than the AC contribution. We are convinced that single layers of Py under FMR condition exhibit the MCP effect because (a) Py has a strong spin-orbit interaction and (b) it has an extrinsic structural symmetry breaking perpendicular to its plane that manifests in the surface magnetic anisotropy, H_S. This enters in the expression for the FMR frequency of thin films in-plane magnetized as $f = \gamma[H_R(H_R + 4\pi M_{\rm eff})]^{1/2}$, where the effective magnetization is $4\pi M_{\rm eff} = 4\pi M_S - H_S$, M_S being the saturation magnetization, $H_S = 2K_S/(M_S t_{Py})$, and K_S is the surface anisotropy constant [25]. As shown in Fig. 3(a), the FMR field shifts considerably with decreasing t_{Py} as a result of the perpendicular anisotropy field. Figure 3(b) shows the data for H_S and the fit $\propto t_{Py}^{-1}$. Surprisingly, the effect of the perpendicular symmetry breaking at the surface can be detected for thicknesses as high as 30 nm, as also reported in Ref. [26]. It means that this effect might be enough to activate the MCP effect in our films. As pointed out in several papers [27,28], the Rashba spin-orbit coupling (RSOC) plays an important role on the origin of the surface anisotropy in thin films of ferromagnetic materials. Besides being associated with the origin of the surface anisotropy in the permalloy films, the RSOC can also be the associated with the origin of the magnonic charge pumping (MCP) effect measured in the same materials. The precondition for the existence of RSOC is a structural inversion symmetry breaking, which is naturally present at any material surface or interface. The other condition for the origin of RSOC is the emergence of materials with high spin-orbit interaction (SOI). This condition is fulfilled by permalloy, which has been shown to exhibit substantial SOI [15]. The major arguments used to justify the argument that RSOC is the basic interaction giving

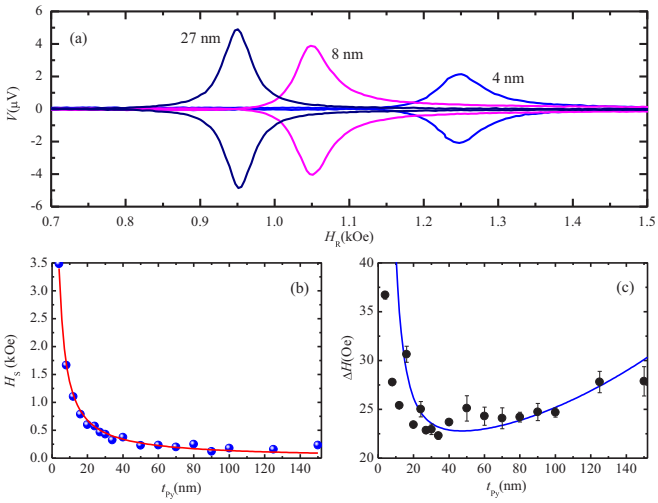

FIG. 3. (Color online) (a) DC voltages measured in three different samples for $\phi_0 = 0^\circ$ confirming the effect of the perpendicular anisotropy field on shifting the resonance and increasing the FMR line width. (b) Dependence of the surface anisotropy field as a function of $t_{\rm Py}$, extracted from the FMR field measured for each sample. The solid line was obtained by fitting with an equation $\propto t_{Py}^{-1}$. (c) Dependence of the FMR line width as a function of the $t_{\rm Py}$. Solid line was obtained as discussed in the text.

rise to the perpendicular anisotropy field and consequently to the MCP in single Py layers were explicitly provided in Refs. [27] and [28]. As all metals, except gold and Pt, possess a natural oxide layer on the surface at room temperature, we can assume that our permalloy films have a native oxide layer on top of the surface. This oxide layer gives rise to charge density gradient, thus generating an electric field perpendicular to the sample surface, which gives rise to RSOC [29]. Both Refs. [27] and [28] come to similar conclusions. In Ref. [27] the perpendicular magnetic anisotropy energy was shown to be given by $E_a \propto -M_S\alpha_r^2\cos^2\theta$ and the surface magnetic anisotropy effective field was shown to be given by $\vec{H}_{\rm eff} \propto \alpha_r^2\cos\theta\,\hat{z}$. Here $\alpha_{\rm r}$ is the Rashba parameter, and θ is the angle that the magnetization vector $\vec{M}_S$ makes with the perpendicular direction $\hat{z}$. Therefore, the Rashba spin-orbit coupling due to the symmetry-broken electric potential at the magnetic surface gives rise to a perpendicular magnetic anisotropy.

As our samples have lateral dimensions 4.0 mm by 1.5 mm, they do not satisfy the condition of quasiunidimensional DC voltage generation verified in the results reported in Refs. [10,11,14]. In the model developed here we extend the previous model [13] and consider that the electric current generated by the time-dependent magnetization can be given by $\vec{j}_e = \vec{j}_e^{(SRE)} + \vec{j}_e^{(MCP)}$, where $\vec{j}_e^{(SRE)}$ is the contribution to the electric current due to the SRE, and $\vec{j}_e^{(MCP)}$ is the contribution to the electric current due to the magnetic charge pumping mechanism. As we pointed out, it is necessary to consider that the electrical current has a component along the z' direction, in addition to the direction of measurement x'. It is important to emphasize that the rf electric current mentioned above is induced by the rf magnetization precession, not due to the external rf electric field, which is assumed to be negligible due to the fact that sample is placed in a nodal position of the rectangular cavity. The time-independent voltages and currents generated by FMR in FM metal films, as results of the spin rectification, are due to the coupling of the rf electric and magnetic field as a consequence of the nonlinear terms in the generalized Ohm's law [14,23],

$$\sigma\vec{E} = \vec{j}_e + \left(\frac{\sigma\Delta\rho}{M_S^2}\right)(\vec{M}\cdot\vec{j}_e)\,\vec{M} - R\sigma\,\vec{j}_e\times\vec{M}, \qquad (1)$$

where σ is the electrical conductivity, $\vec{j}_e$ is the current density, the second term on the right is due to the anisotropic contributions to the resistivity [Anisotropic Magnetoresistance (AMR) and Planar Hall Effect (PHE)], $\Delta\rho = \rho_{//} - \rho_\perp$, M_S is the saturation magnetization, and R is the extraordinary Hall coefficient. By introducing the oscillating components of the magnetization $\vec{m}$ such that $\vec{M} = \vec{M}_z + \vec{m}$, and retaining only linear terms in Eq. (1), after taking the time average, the time-independent electric field is found to be

$$\vec{E}_0 = -\left(\frac{\Delta\rho}{M_S^2}\right)[2\langle\vec{m}\cdot\vec{j}_e\rangle\,\vec{M}_z + \langle\vec{j}_e\times\vec{m}\rangle\times\vec{M}_z] + R\,\langle\vec{j}_e\times\vec{m}\rangle. \qquad (2)$$

For the microwave fields, we only need to find the average expressions: $\langle\vec{m}\cdot\vec{j}_e\rangle$ and $\langle\vec{j}_e\times\vec{m}\rangle$. Taking into account the reference frame of the sample as $x'z'$ of Fig. 1(b), the magnetization and magnetic fields are written as $\vec{H}_0' = (-H_0\sin\phi_0, 0, H_0\cos\phi_0)$, $\vec{h}' = (h(t)\cos\phi_0, 0, h(t)\sin\phi_0)$, $\vec{M}_0' = (-M_S\sin\phi_0, 0, M_S\cos\phi_0)$, $\vec{m}'(t) = (m_x(t)\cos\phi_0, m_y, m_x(t)\sin\phi_0)$. Thus the electrical current density, including the magnetic charge pumping contribution $j_z^{(MCP)}$ in the $x'z'$ plane can be written as

$$\vec{j}_e' = \left[\left(j_{ex'} - j_z^{(MCP)}\right)\sin\phi_0,\, 0,\, \left(-j_{ez'} + j_z^{(MCP)}\right)\cos\phi_0\right], \qquad (3)$$

where $j_{ex'}$ and $j_{ez'}$ are the components of the current density along axes x' and z', due to the anisotropic contributions, and $j_z^{(MCP)}$ is the component of the current density along the z axis, due to the magnonic charge pumping mechanism. Following the approach developed in Ref. [22], $j_z^{(MCP)}$ is proportional to $\partial m_x/\partial t$ and $\partial m_y/\partial t$ and is given by $j_z^{(MCP)} = (\Lambda^{(r)}/M_S)\partial m_x/\partial t + (\Lambda^{(d)}/M_S)\partial m_y/\partial t$, where $\Lambda^{(r)}$ and $\Lambda^{(d)}$ represent the reactive and dissipative charge pumping process. By using $M_0 \approx M_S$ and m_x and m_y as the rf components along x and y directions, respectively, the x' component of the electric field can be written as

$$\vec{E}_0'\cdot\hat{x}' = -\left(\frac{\Delta\rho}{M_S}\right)\Big[-\frac{3}{2}\langle m_x j_{ex'}\rangle\sin\phi_0\sin 2\phi_0 + \frac{3}{2}\langle m_x j_{ez'}\rangle\sin\phi_0\sin 2\phi_0\Big] + \left(\frac{\Delta\rho}{M_S}\right)\Big[\left(\langle m_x j_{ez'}\rangle + \langle m_x j_z^{(MCP)}\rangle\right)\cos\phi_0\Big]. \qquad (4)$$

Here we disregard the contribution from the anomalous Hall Effect, which points perpendicular to the plane spanned by the vectors $\vec{j}_e$ and $\vec{M}$. The voltage measured along the x' direction can be calculated as $V_{FMR} = \int_{-w_{FM}/2}^{w_{FM}/2}\vec{E}_0'\cdot\hat{x}'\,dx'$, where $w_{\rm FM}$

is the length of the ferromagnetic layer. Thus,

$$V_{FMR} = \left(\frac{\Delta\rho}{M_S}\right) w_{FM}\Big[\Big(\frac{3}{2}\langle(j_{ex'} - j_{ez'})m_x\rangle\Big)\sin(2\phi_0)\sin(\phi_0) + \big(\langle(j_{ez'}m_x\rangle + \langle(j_z^{(MCP)}m_x\rangle\big)\cos(\phi_0)\Big]. \quad (5)$$

Here the components of the current density can be written as

$$j_e = |j_e|e^{i\omega t} \text{and} j_z^{(MCP)} = i\frac{\omega\Lambda^{(r)}}{M_S}m_x(t) + i\frac{\omega\Lambda^{(d)}}{M_S}m_y(t), \quad (6)$$

and the transverse components of the magnetization, m_x and m_y, are obtained by solving the Landau-Lifshitz-Gilbert equation, which are related to the transverse rf field $\vec{h}$ through the following equations:

$$m_x(t) = A_{xx}h_x\frac{\Delta H}{\sqrt{(H-H_R)^2+\Delta H^2}}e^{i\,\omega t}e^{i\,(\Phi-\Theta)}, \quad (7)$$

$$m_y(t) = -iA_{xy}h_x\frac{\Delta H}{\sqrt{(H-H_R)^2+\Delta H^2}}e^{i\,\omega t}e^{i\,(\Phi-\Theta)}, \quad (8)$$

where $A_{xx} = \frac{M(H+4\pi M_{\text{eff}})}{\Delta H_G(2H+4\pi M_{\text{eff}})}$, $A_{xy} = \frac{M\omega}{\gamma\Delta H_G(2H+4\pi M_{\text{eff}})}$ and $\Delta H = \frac{\Delta H_G(2H+4\pi M_{\text{eff}})}{(H+H_R+4\pi M_{\text{eff}})}$. Here M_{eff} is the effective magnetization, H_r is the resonance field and, ΔH_G is the Gilbert contribution to the line width. Φ is the relative phase shift between the rf electric and magnetic fields and Θ the phase between $\vec{m}$ and $\vec{h}$ that satisfy the following equations:

$$\sin\Theta = \frac{\Delta H}{\sqrt{(H-H_R)^2+\Delta H^2}}, \quad (9)$$

$$\cos\Theta = \frac{(H-H_r)}{\sqrt{(H-H_R)^2+\Delta H^2}}. \quad (10)$$

The time average values appearing in Eq. (5), $\langle j_{ex'}m_x\rangle = \langle \text{Re}\, j_{ex'}\text{Re}m_x\rangle$ and $\langle j_{ex'}m_x\rangle = \langle \text{Re}\, j_{ex'}\text{Re}m_x\rangle$ are given by

$$\begin{aligned}\langle j_{ex'}m_x\rangle &= \frac{I_{rfx'}}{2t_{FM}w_{FM}}A_{xx}h_x\frac{\Delta H}{\sqrt{(H-H_R)^2+\Delta H^2}}\\ &\quad\times\cos(\Phi-\Theta)\\ &= \frac{I_{rfx'}}{2t_{FM}w_{FM}}A_{xx}h_x\Big[\frac{\Delta H(H-H_r)}{(H-H_R)^2+\Delta H^2}\cos\Phi\\ &\quad+\frac{\Delta H^2}{(H-H_R)^2+\Delta H^2}\sin\Phi\Big], \quad (11)\end{aligned}$$

$$\begin{aligned}\langle j_{ez'}m_x\rangle &= \frac{I_{rfz'}}{2t_{FM}l_{FM}}A_{xx}h_x\frac{\Delta H}{\sqrt{(H-H_R)^2+\Delta H^2}}\\ &\quad\times\cos(\Phi-\Theta)\\ &= \frac{I_{rfz'}}{2t_{FM}w_{FM}}A_{xx}h_x\Big[\frac{\Delta H(H-H_r)}{(H-H_R)^2+\Delta H^2}\cos\Phi\\ &\quad+\frac{\Delta H^2}{(H-H_R)^2+\Delta H^2}\sin\Phi\Big]. \quad (12)\end{aligned}$$

On the other hand,

$$\begin{aligned}\langle j_z^{(MCP)}m_x\rangle &= \langle \text{Re}\, j_z^{(MCP)}\text{Re}m_x\rangle\\ &= -\frac{\omega\Lambda^{(r)}}{M_S}|m_x|^2\langle\sin(\omega t+\Phi-\Theta)\cdot\\ &\quad\times\cos(\omega t+\Phi-\Theta)\rangle + \frac{\omega\Lambda^{(d)}}{M_S}|m_x||m_y|\\ &\quad\times\langle\cos(\omega t+\Phi-\Theta)\cdot\cos(\omega t+\Phi-\Theta)\rangle. \quad (13)\end{aligned}$$

Note that the time average of the part containing the reactive term of the MCP current is zero, then

$$\langle j_z^{(MCP)}m_x\rangle = \frac{A_{xy}A_{xx}\Lambda^{(d)}\omega h_x^2}{2M_S}\Big[\frac{\Delta H^2}{(H-H_R)^2+\Delta H^2}\Big]. \quad (14)$$

By plugging the time averages calculated above into Eq. (5) the voltage measured along the x' direction is given by

$$\begin{aligned}V_{FMR} &= A\Big[\frac{\Delta H(H-H_r)}{(H-H_R)^2+\Delta H^2}\cos\Phi\\ &\quad+\frac{\Delta H^2}{(H-H_R)^2+\Delta H^2}\sin\Phi\Big]\sin\phi_0\sin(2\phi_0)\\ &\quad+B\Big[\frac{\Delta H(H-H_r)}{(H-H_R)^2+\Delta H^2}\cos\Phi\\ &\quad+\frac{\Delta H^2}{(H-H_R)^2+\Delta H^2}\sin\Phi\Big]\cos\phi_0\\ &\quad+\frac{\Delta\rho}{2M_S^2}w_{FM}A_{xy}A_{xx}\Lambda^{(d)}\omega h_x^2\\ &\quad\times\Big[\frac{\Delta H^2}{(H-H_R)^2+\Delta H^2}\Big]\cos\phi_0, \quad (15)\end{aligned}$$

with $A = \frac{\Delta\rho}{2M_S}\frac{I_{rfx'}}{t_{FM}}A_{xx}h_x$ and $B = \frac{\Delta\rho}{2M_S}\frac{I_{rfz'}}{t_{FM}}A_{xx}h_x$, and $I_{rfx'}$ and $I_{rfz'}$ are the rf currents along the x' and z' directions, respectively. The first and second terms in Eq. (15) arise from the anisotropic contributions and the last term accounts for the MCP contribution.

Equation (15) can be written in a more compact form as

$$\begin{aligned}V_{FMR}(\phi_0,H) &= [A\sin\Phi\sin\phi_0\sin(2\phi_0) + B\sin\Phi\cos\phi_0\\ &\quad+V_{\text{MCP}}\cos\phi_0]\,L + [A\cos\Phi\sin\phi_0\\ &\quad\times\sin(2\phi_0) + B\cos\Phi\cos\phi_0]\,D, \quad (16)\end{aligned}$$

where $L = \Delta H^2/[(H-H_r)^2+\Delta H^2]$ is the Lorentz line shape, and $D = \Delta H(H-H_r)/([(H-H_r)^2+\Delta H^2]$ is the dissipative antisymmetric line shape, Φ is the angle between the rf magnetic field and the induced rf electric field, and the coefficients A and B depend on the rf current and the magnetic parameters of the FM film. The component due to the MCP is written as

$$\begin{aligned}V_{\text{MCP}} &= \frac{\Delta\rho}{2M_S^2}w_{FM}A_{xy}A_{xx}\Lambda^{(d)}\omega h_x^2\\ &\cong\frac{\Delta\rho\,w_{FM}}{2M_s^2}\frac{M_{\text{eff}}\gamma}{4\pi\alpha^2}\Lambda^{(d)}h_x^2. \quad (17)\end{aligned}$$

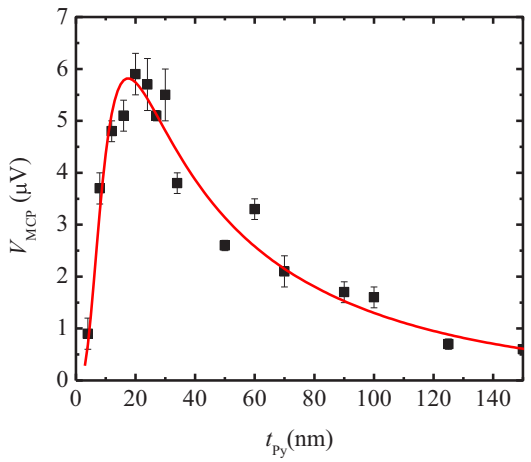

FIG. 4. (Color online) V_{MCP} data (solid squares) extracted from the measurements by means of the equation $V_{MCP} = b_{sym}[1 - (a_{sym}/b_{sym})(b_{antisym}/a_{antisym})]$. The solid line was obtained by using Eq. (17) in which we used the experimental data for the effective magnetization (M_{eff}) and the Gilbert damping (α).

Here α $(= \gamma \Delta H/\omega)$ is the Gilbert damping. Equation (16) can be written as $V_{FMR}(\phi_0, H) = A_{sym}(\phi_0, H) + B_{antisym}(\phi_0, H)$, where for each angle ϕ_0 the symmetric contribution is $A_{sym}(\phi_0, H) = a_{sym} \sin\phi_0 \sin(2\phi_0) + b_{sym} \cos\phi_0$, and the antisymmetric is $B_{antisym}(\phi_0, H) = a_{antisym} \sin\phi_0 \sin(2\phi_0) + b_{antisym} \cos\phi_0$, where $a_{sym} = A \sin\Phi$, $b_{sym} = B \sin\Phi + V_{MCP}$, $a_{antisym} = A \cos\Phi$, and $b_{antisym} = B \cos\Phi$. From these equations we can obtain the contribution from the MCP effect as $V_{MCP} = b_{sym}[1 - (a_{sym}/b_{sym})(b_{antisym}/a_{antisym})]$. In order to exemplify how to obtain the MCP contribution, from the numerical fits of the sample with thickness $t_{Py} = 34$ nm, Fig. 2(d), we obtain $a_{sym} = 4.3 \pm 0.3\,\mu$V, $b_{sym} = 3.4 \pm 0.2\,\mu$V, $a_{antisym} = 16.1 \pm 0.8\,\mu$V, and $b_{antisym} = -1.3 \pm 0.5\,\mu$V, so $V_{MCP} = 3.8 \pm 0.2\,\mu$V. With this value, from Eq. (17) we calculate the value of $\Lambda^{(d)}$. Considering an AMR for Py of 2% and estimating the magnitude of the rf magnetic field as $h_x \sim 0.4$ Oe corresponding to an incident microwave power of 40 mW, we obtain $\Lambda^{(d)} \sim 7 \times 10^{-6}\,\mathrm{A\,s\,cm^{-2}}$. The parameter characterizing the SOT ($\eta^{(d)}$) can be obtained directly from the reciprocity relation $\eta^{(d)} = \rho \frac{\Lambda^{(d)}}{M_S}$ deduced in Ref. [22]. Then for the sample in consideration we obtain $\eta^{(d)} = 2 \times 10^{-9}\,\mathrm{T\,A^{-1}\,cm^{-2}}$, which is one order of magnitude larger than the value reported in Ref. [30] for the reactive SOT in ferromagnetic heterostructures $Pt/Co/AlO_x$.

From the measurements of the whole set of samples we were able to obtain the MCP contribution to the DC voltage measured for each sample. Figure 4 shows the dependence of V_{MCP} as a function of t_{Py} (solid squares). The solid line was obtained by using Eq. (17) considering the experimental data of $M_{eff}(t_{Py})$ and $\alpha(t_{Py})$ as a function of the Py thickness and considering that $\Lambda^{(d)} \propto 1/t_{FM}$ as expected [31]. The measured dependence of the FMR line width as a function of t_{Py} is shown in Fig. 3(c). As the damping parameter $\alpha(t_{Py})$,$[\alpha = (\gamma/\omega)\Delta H]$ plays a crucial role on the behavior of V_{MCP} we used an equation for the FMR line width given by $\Delta H = \Delta H_G + \Delta H_{2M} + \Delta H_{eddy}$. Here ΔH_G is the intrinsic contribution value ($\Delta H_G = 21$Oe), ΔH_{2M} is the two-magnon scattering contribution ($\Delta H_{2M} = C' H_S^2 = C_{2M}/t_{Py}^2$)(see Ref. [32]), and the eddy current contribution ($\Delta H_{eddy} = C_{eddy} t_{Py}^2$) is important in the high-thickness regime (see Ref. [33]). The solid line shown in Fig. 3(c) was obtained by using $C_{2M} = 2.0\,\mathrm{Oe} \times \mathrm{nm}^2$ [2] and $C_{eddy} = 4.0 \times 10^{-7}\mathrm{Oe/nm}^2$. As observed, the contribution of the MCP effect to the DC voltage exhibits two different regimes, as a function of the Py layer thickness. In the first regime that corresponds to thicknesses ranging from 4.0 nm to 30 nm, V_{MCP} increases linearly up to thicknesses around 30 nm. This is the regime of thicknesses in which the surface perpendicular anisotropy field is operative and is responsible for the symmetry breaking normal to the films. In the second regime that corresponds to thicknesses larger than 30 nm, the layers are thick enough and the perpendicular anisotropy field does not play an important role anymore. Our data clearly show that the effect reported here is of interface origin mostly due to the surface anisotropy field, as seen in Figs. 3(b), 3(c), and 4.

IV. CONCLUSIONS

In conclusion, we measured the DC voltage generated in single layers of permalloy undergoing FMR for a set of samples in which the thickness varied from 4 to 150 nm. For each sample, we measured the in-plane DC voltage that exhibits asymmetrical line shapes, which are explained by a superposition of symmetric and antisymmetric Lorentzian curves. The angular dependence of both contributions cannot be explained by spin rectification effects only. We have developed a model in which a contribution from the magnonic charge pumping effect has been added. The MCP effect that has been recently discovered as the reciprocal of the spin orbit torque effect converts magnetization dynamics in charge accumulation by means of the spin orbit interaction. In our films we have shown a perpendicular anisotropy field that arises due to the symmetry breaking at the surface of the films can support the origin of the MCP effect.

ACKNOWLEDGMENT

Research was supported in Brazil by the agencies CNPq, CAPES, FINEP, and FACEPE, in Mexico by CONACYT, and in Chile by FONDECYT No. 1130705.

[1] D. C. Ralph and M. D. Stiles, J. Magn. Magn. Mater. **320**, 1190 (2008).

[2] Y. Tserkovnyak, A. Brataas, and G. E. W. Bauer, Phys. Rev. Lett. **88**, 117601 (2002).

[3] S. Mizukami, Y. Ando, and T. Miyazaki, Phys. Rev. B **66**, 104413 (2002).

[4] B. Heinrich, Y. Tserkovnyak, G. Woltersdorf, A. Brataas, R. Urban, and G. E. W. Bauer, Phys. Rev. Lett. **90**, 187601 (2003).

[5] A. Azevedo, L. H. Vilela Leão, R. L. Rodriguez-Suarez, A. B. Oliveira, and S. M. Rezende, J. Appl. Phys. **97**, 10C715 (2005).
[6] E. Saitoh, M. Ueda, H. Miyajima, and G. Tatara, Appl. Phys. Lett. **88**, 182509 (2006).
[7] J. E. Hirsch, Phys. Rev. Lett. **83**, 1834 (1999).
[8] S. S.-L. Zhang, K. Chen, and S. Zhang, Europhys. Lett. **106**, 67007 (2014).
[9] M. V. Costache, M. Sladkov, S. M. Watts, C. H. van der Wal, and B. J. van Wees, Phys. Rev. Lett. **97**, 216603 (2006).
[10] Y. S. Gui, N. Mecking, X. Zhou, G. Williams, and C. -M. Hu, Phys. Rev. Lett. **98**, 107602 (2007).
[11] O. Mosendz, V. Vlaminck, J. E. Pearson, F. Y. Fradin, G. E. W. Bauer, S. D. Bader, and A. Hoffmann, Phys. Rev. B **82**, 214403 (2010).
[12] L. Liu, T. Moriyama, D. C. Ralph, and R. A. Buhrman, Phys. Rev. Lett. **106**, 036601 (2011).
[13] A. Azevedo, L. H. Vilela-Leão, R. L. Rodríguez-Suárez, A. F. Lacerda Santos, and S. M. Rezende, Phys. Rev. B **83**, 144402 (2011).
[14] M. Harder, Z. X. Cao, Y. S. Gui, X. L. Fan, and C.-M. Hu, Phys. Rev. B **84**, 054423 (2011).
[15] B. F. Miao, S. Y. Huang, D. Qu, and C. L. Chien, Phys. Rev. Lett. **111**, 066602 (2013).
[16] A. Azevedo, O. Alves Santos, G. A. Fonseca Guerra, R. O. Cunha, R. Rodríguez-Suárez, and S. M. Rezende, Appl. Phys. Lett. **104**, 052402 (2014).
[17] A. Tsukahara, Y. Ando, Y. Kitamura, H. Emoto, E. Shikoh, M. P. Delmo, T. Shinjo, and M. Shiraishi, Phys. Rev. B **89**, 235317 (2014).
[18] A. Azevedo, O. Alves Santos, R. O. Cunha, R. Rodríguez-Suárez, and S. M. Rezende, Appl. Phys. Lett. **104**, 152408 (2014).
[19] I. M. Miron, T. Moore, H. Szambolics *et al.*, Nat. Mater. **10**, 419 (2011).
[20] I. M. Miron, K. Garello, G. Gaudin, P. J. Zermatten, M. V. Costache, S. Auffret, S. Bandiera, B. Rodmacq, A. Schuhl, and P. Gambardella, Nature (London) **476**, 189 (2011).
[21] J. C. Rojas Sánchez, L. Vila, G. Desfonds, S. Gambarelli, J. P. Attané, J. M. De Teresa, C. Magén, and A. Fert, Nat. Commun. **4**, 2944 (2013).
[22] C. Ciccarelli, K. M. D. Hals, A. Irvine, V. Novak, Y. Tserkovnyak, H. Kurebayashi, A. Brataas, and A. Ferguson, Nat. Nanotech. **10**, 50 (2015).
[23] W. G. Egan and H. J. Juretschke, J. Appl. Phys. **34**, 1477 (1963).
[24] N. Mecking, Y. S. Gui, and C.-M. Hu, Phys. Rev. B **76**, 224430 (2007).
[25] B. Heinrich and J. F. Cochran, Adv. Phys. **42**, 523 (1993).
[26] J. P. Nibarger, R. Lopusnik, Z. Celinski, and T. J. Silva, Appl. Phys. Lett. **83**, 93 (2003).
[27] L. Xu and S. Zhang, J. Appl. Phys. **111**, 07C501 (2012).
[28] S. E. Barnes, J. Ieda, and S. Maekawa, Sci. Rep. **4**, 4105, (2014).
[29] O. Krupin, G. Bihlmayer, K. Starke, S. Gorovikov, J. E. Prieto, K. Döbrich, S. Blügel, and G. Kaindl, Phys. Rev. B **71**, 201403(R) (2005).
[30] K. Garello, I. M. Miron, C. O. Avci, F. Freimuth, Y. Mokrousov, S. Blugel, S. Auffret, O. Boulle, G. Gaudin, and P. Gambardella, Nat. Nanotech. **8**, 587 (2013).
[31] X. Fan, H. Celik, J. Wu, C. Ni, K.-J. Lee, V. O. Lorenz, and J. Q. Xiao, Nat. Commun. **5**, 3042 (2014).
[32] A. Azevedo, A. B. Oliveira, F. M. de Aguiar, and S. M. Rezende, Phys. Rev. B **62**, 5331 (2000).
[33] B. Heinrich, R. Urban, and G. Woltersdorf, J. Appl. Phys. **91**, 7523 (2002).